Protein phosphatase 4 controls circadian clock dynamics by modulating CLOCK/BMAL1 activity

Sabrina Klemz[1,4], Thomas Wallach[1,4], Sandra Korge[1], Mechthild Rosing[3], Roman Klemz[1], Bert Maier[1], Nicholas C. Fiorenza[1], Irem Kaymak[1], Anna K. Fritzsche[1], Erik D. Herzog[2], Ralf Stanewsky[3], Achim Kramer[1*]

[1] Charité –Universitätsmedizin Berlin, corporate member of Freie Universität Berlin and Humboldt-Universität zu Berlin, Laboratory of Chronobiology, Charitéplatz 1, 10117 Berlin, Germany
[2] Department of Biology, Washington University in St. Louis, St. Louis, MO 63130
[3] Institute of Neuro and Behavioral Biology, Westfälische Wilhelms University, Münster 48149, Germany
[4] These authors contributed equally

[*] correspondence: achim.kramer@charite.de

Supplemental Note, Figures and Tables

Supplemental Note

Rhythmic transcription of *BMAL1* is achieved by the orphan nuclear receptors RORα/β/γ (ROR activators) and REV-ERBα/β (REV-ERB repressors) via competitive binding to RRE elements (ROR response elements) in the promoter of *BMAL1*. For efficient repressor activity, REV-ERBs additionally associate with co-repressors N-CoR1 and HDAC3 (Feng et al., 2011; Yin and Lazar, 2005).

Moreover, PPP4 inhibits HDAC3 activity by dephosphorylating a specific phosphorylation site (Zhang et al, 2005). Accordingly, reduced PPP4C expression (e.g., by RNAi-mediated knockdown) would lead to stronger HDAC3 activity and could thus enhance the repressor activity REV-ERBs at the *BMAL1* promoter. Thus, the reduced BMAL1 expression of PPP4C-depleted cells (**Fig. 2A**) could be explained by this mechanism. However, such a mechanism would also predict higher BMAL1 transcript levels with PPP4C overexpression, which we did not observe (**Fig. 2B**).

To test whether PPP4 modulates the transcriptional activity of RREs, we performed a transactivation assay in HEK293 cells with a reporter construct expressing luciferase under the control of six tandem RREs. As expected, coexpression of RORγ increased luciferase signaling and the known repressor REV-ERBα with and without additional HDAC3 reduced it. Co-expression of PPP4C, but not the catalytically inactive mutant, enhanced transcriptional activity under all conditions, suggesting that PPP4 activity can positively modulate transcriptional activity at RREs (**Supplemental Fig. S3A**).

If the modulatory activity of PPP4 in transcription at RREs (via the described dephosphorylation of HDAC3) is causative for the circadian period phenotype observed upon depletion of *PPP4*, then this phenotype should be significantly attenuated in cells lacking HDAC3. We therefore knocked-down HDAC3 and PPP4 together, but still detected the short-period phenotype, which also occurred when only PPP4C was depleted (**Supplemental Fig. S3B**).

Taken together, this suggests that although PPP4C activity may modulate transcriptional activity at RREs, this is unlikely to be the cause of the short-period phenotype upon PPP4C depletion.

Supplemental References

Zhang, X. Histone deacetylase 3 (HDAC3) activity is regulated by interaction with protein serine/threonine phosphatase 4. *Genes & Development* **19**, 827–839 (2005).

Feng, D. *et al.* A Circadian Rhythm Orchestrated by Histone Deacetylase 3 Controls Hepatic Lipid Metabolism. *Science* **331**, 1315–1319 (2011).

Yin, L. & Lazar, M. A. The Orphan Nuclear Receptor Rev-erbα Recruits the N-CoR/Histone Deacetylase 3 Corepressor to Regulate the Circadian Bmal1 Gene. **19**, 1452–1459 (2005).

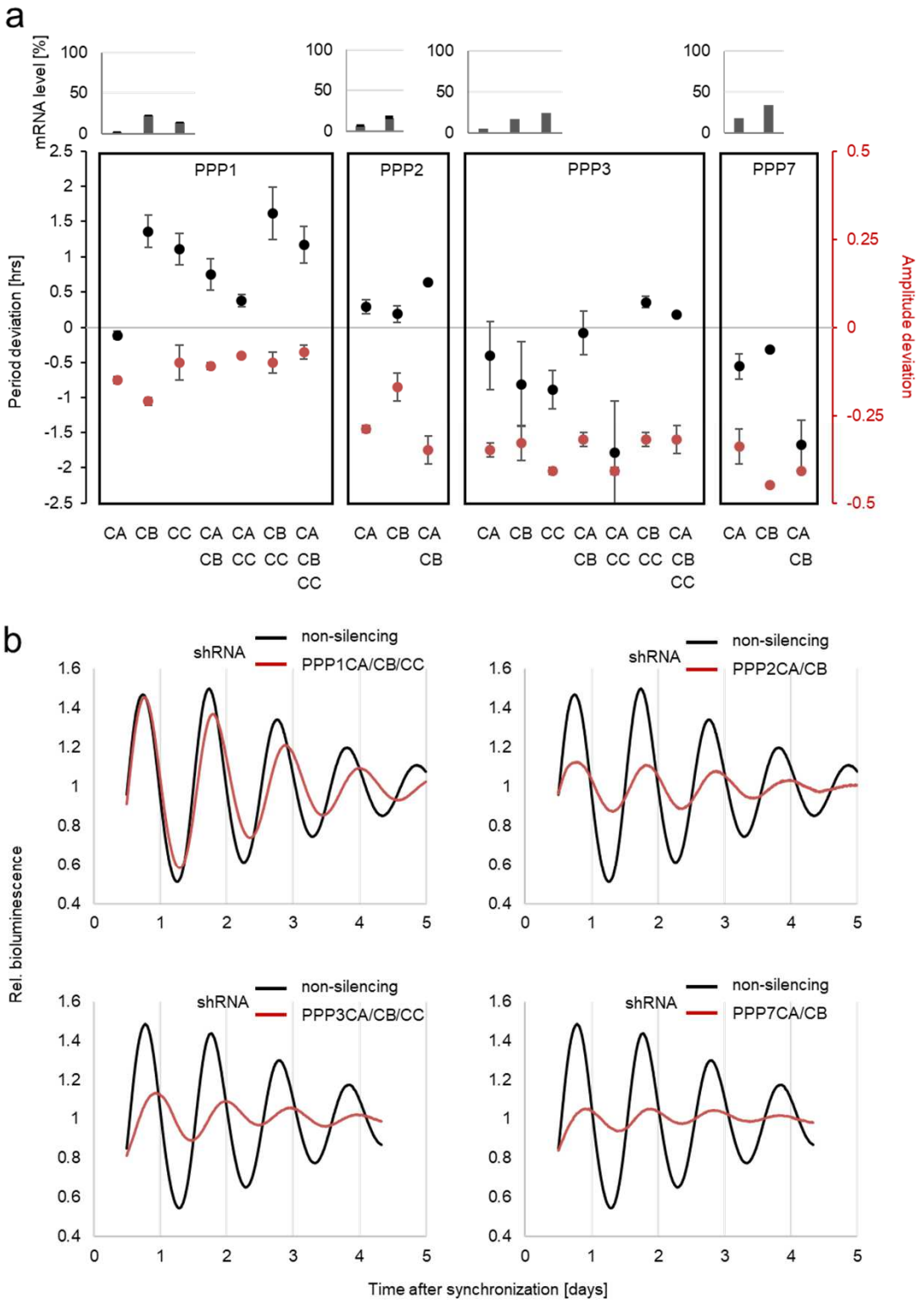

Supplemental Fig. S1. Functional redundancy of the catalytic Ser/Thr phosphatase isoforms in the circadian oscillator. (A) RNAi-based screening in U-2 OS/*Bmal1*-luciferase reporter cells for altered period and amplitude phenotypes of catalytic phosphatase subunits whose isoforms (CA, CB, or CC) were depleted either individually or in the indicated combinations. Each dot represents the period deviation (black circles, primary axis) or amplitude deviation (red circles, secondary axis) from the mean period of the control shRNA of three independent replicates of one experiment ± SD. (Top) The mRNA expression of the catalytic phosphatase subunits after respective depletion relative to the gene expression of control shRNA (for PPP1/PPP2, mean (n=3) ± SD, for PPP3/PPP7 (n=1). **(B)** Trend-eliminated oscillation dynamics of U-2 OS reporter cells lentivirally transduced with shRNA constructs targeting the catalytic subunits of indicated Ser/Thr phosphatases.

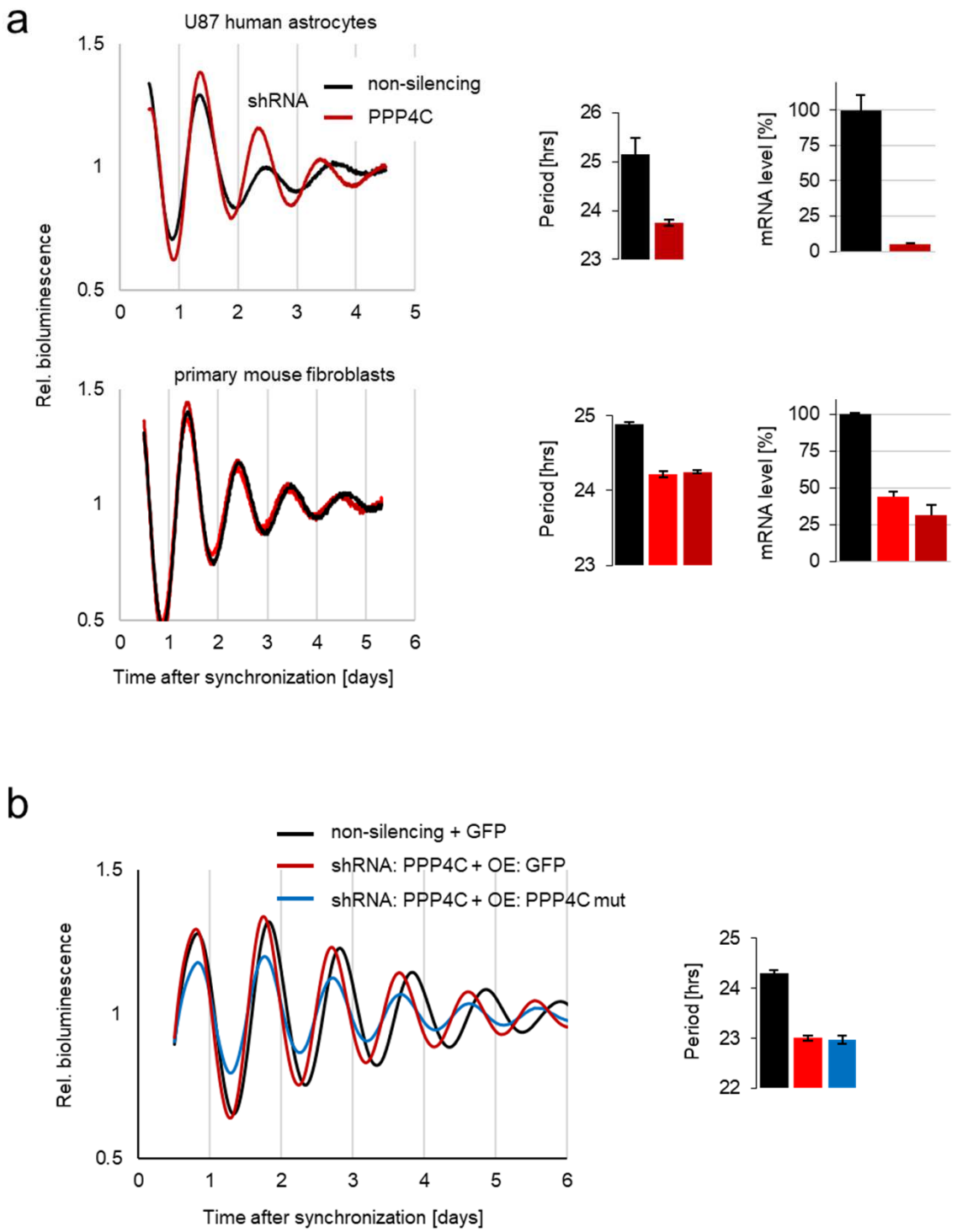

Supplemental Fig. S2. Genetic depletion of PPP4C shortens the circadian period in primary PER2::LUC mouse fibroblasts and the human astrocyte cell line U87. (A) Trend-eliminated oscillation dynamics of primary PER2::LUC mouse fibroblasts or human astrocytes (U87) harboring a *Per2*-luciferase reporter construct upon RNAi-mediated depletion of PPP4C. Given are period of oscillations and efficiency of depletion of PPP4C. Error bars represent the range of two independent replicates of one experiment (fibroblasts) or standard deviation of three independent replicates of one experiment (U87 cells). **(B)** Combining knockdown of endogenous *PPP4C* and overexpression of the catalytically inactive PPP4CA mutant does not further shorten the circadian period. Trend-eliminated oscillation dynamics of U-2 OS/Bmal1 luciferase reporter cells. For depletion of endogenous PPP4C mRNA, an shRNA directed against the 3'-UTR of PPP4C was used. In this background, either tGFP or a catalytically inactive PPP4CA mutant was ectopically overexpressed (OE). Error bars represent the range of two independent replicates of one experiment.

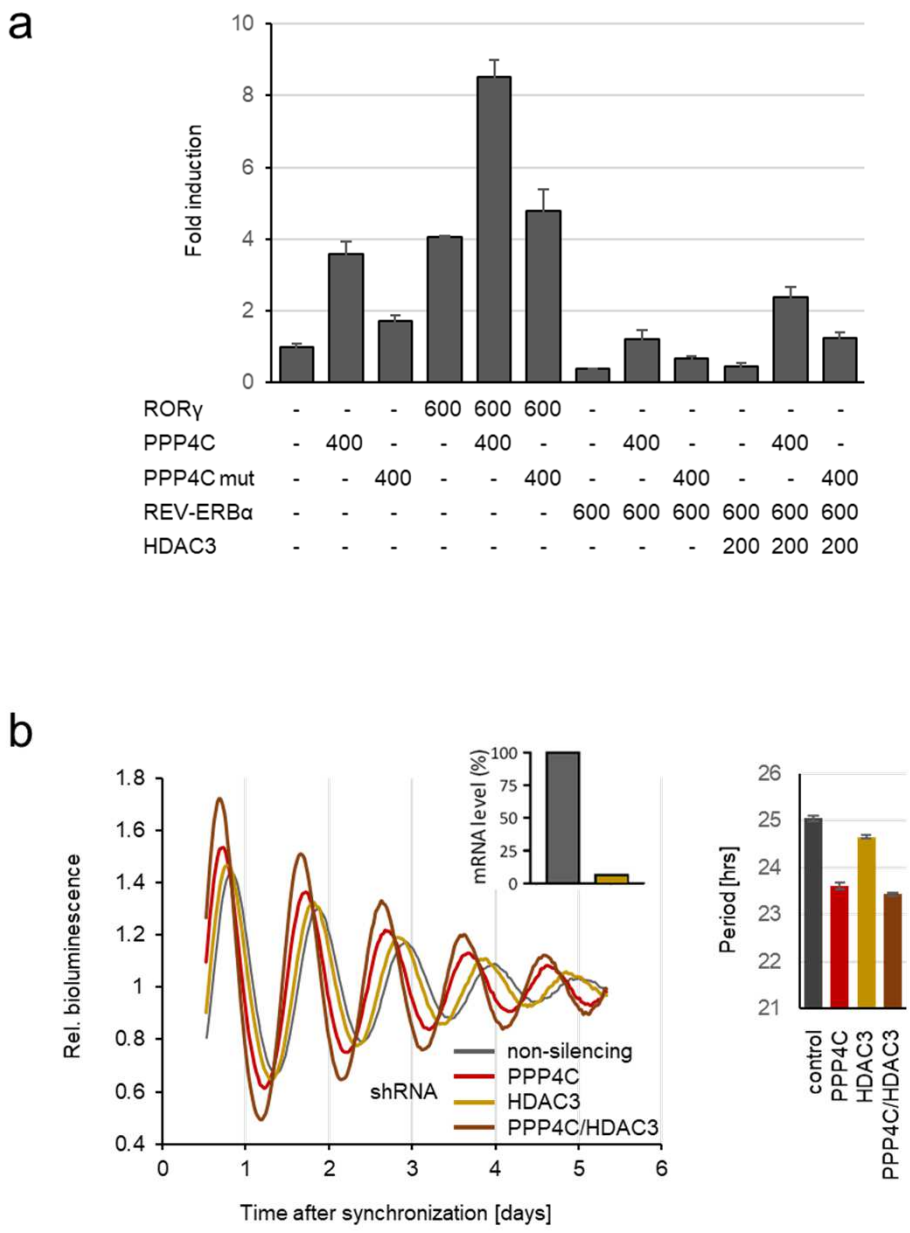

Supplemental Fig. S3. The circadian phenotype upon PPP4 depletion does not depend on HDAC3, although PPP4 modulates transcription from ROR-response elements (RRE). (A). RORγ- and REV-ERBα/HDAC3-mediated transactivation from a six RRE-containing luciferase construct in HEK293 cells. Indicated expression constructs were co-transfected (numbers indicate ng amounts). Shown are means ± SD from three independent samples. **(B)** Left: Trend-eliminated mean oscillation dynamics of U-2 OS reporter cells lentivirally transduced with shRNA constructs targeting *PPP4C*, *HDAC3* or both. Knockdown efficiency of the RNAi-constructs targeting *HDAC3* was quantified using qPCR (inset). Right: Quantification of oscillation periods (n=4, mean ± SD).

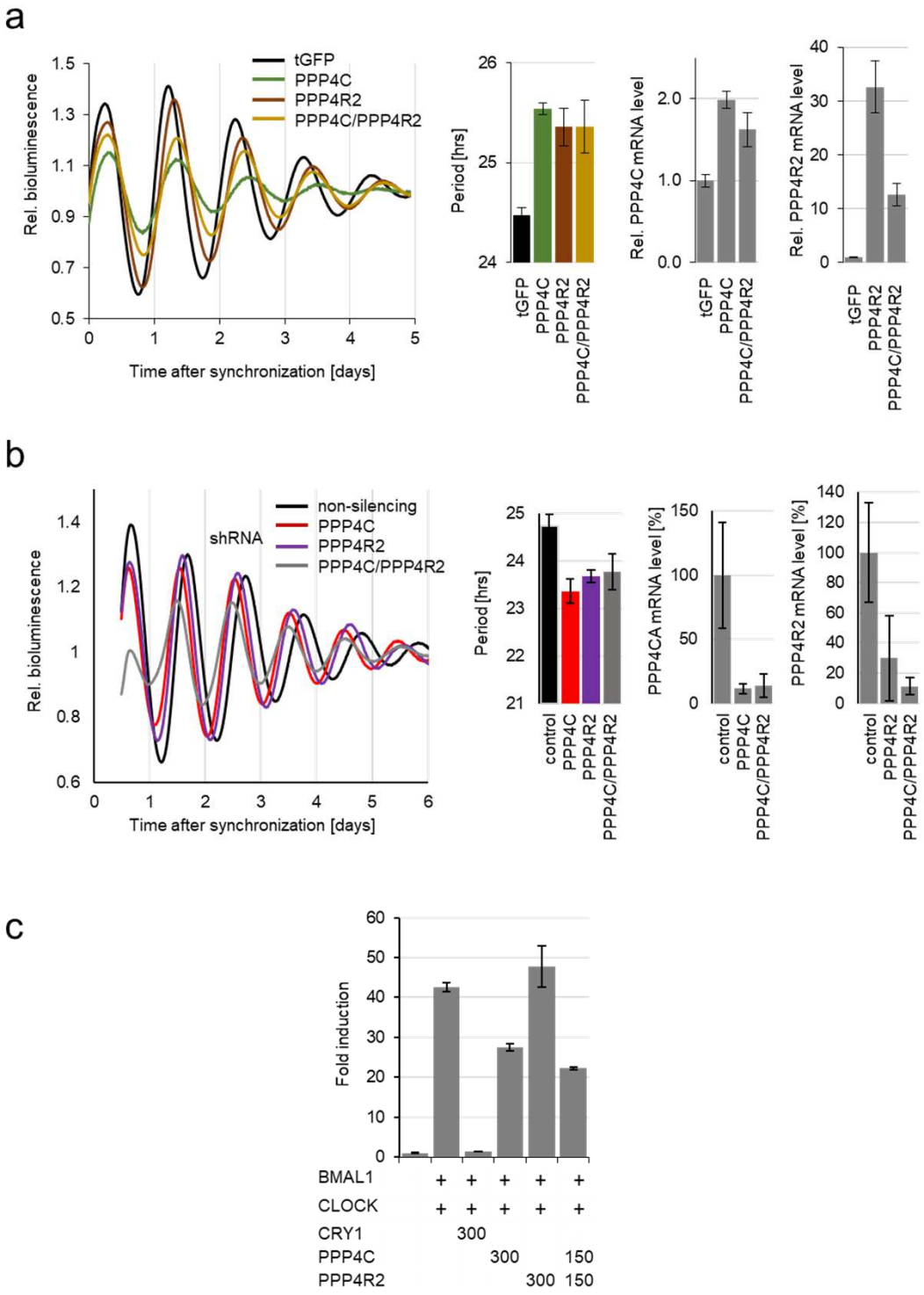

Supplemental Fig. S4. PPP4R2 is the regulatory subunit crucial for normal rhythms in human cells. **(A)** Trend-eliminated oscillation dynamics of U-2 OS reporter cells lentivirally transduced with expression constructs for PPP4C, the regulatory subunit of protein phosphatase 4 PPP4R2, a combination of both or tGFP as an overexpression control. Shown are results from three experiments (mean ± SD). **(B)** Trend-eliminated oscillation dynamics of U-2 OS reporter cells lentivirally transduced with shRNA constructs targeting PPP4C, PPP4R2 or both. Knockdown efficiency was quantified using qPCR. Shown are results from three experiments (mean ± SD). **(C)** CLOCK/BMAL1-mediated transactivation from a six E-boxes containing luciferase construct in HEK293 cells. Indicated expression constructs were co-transfected (numbers indicate ng amounts). Shown are means ± SD from three independent samples.

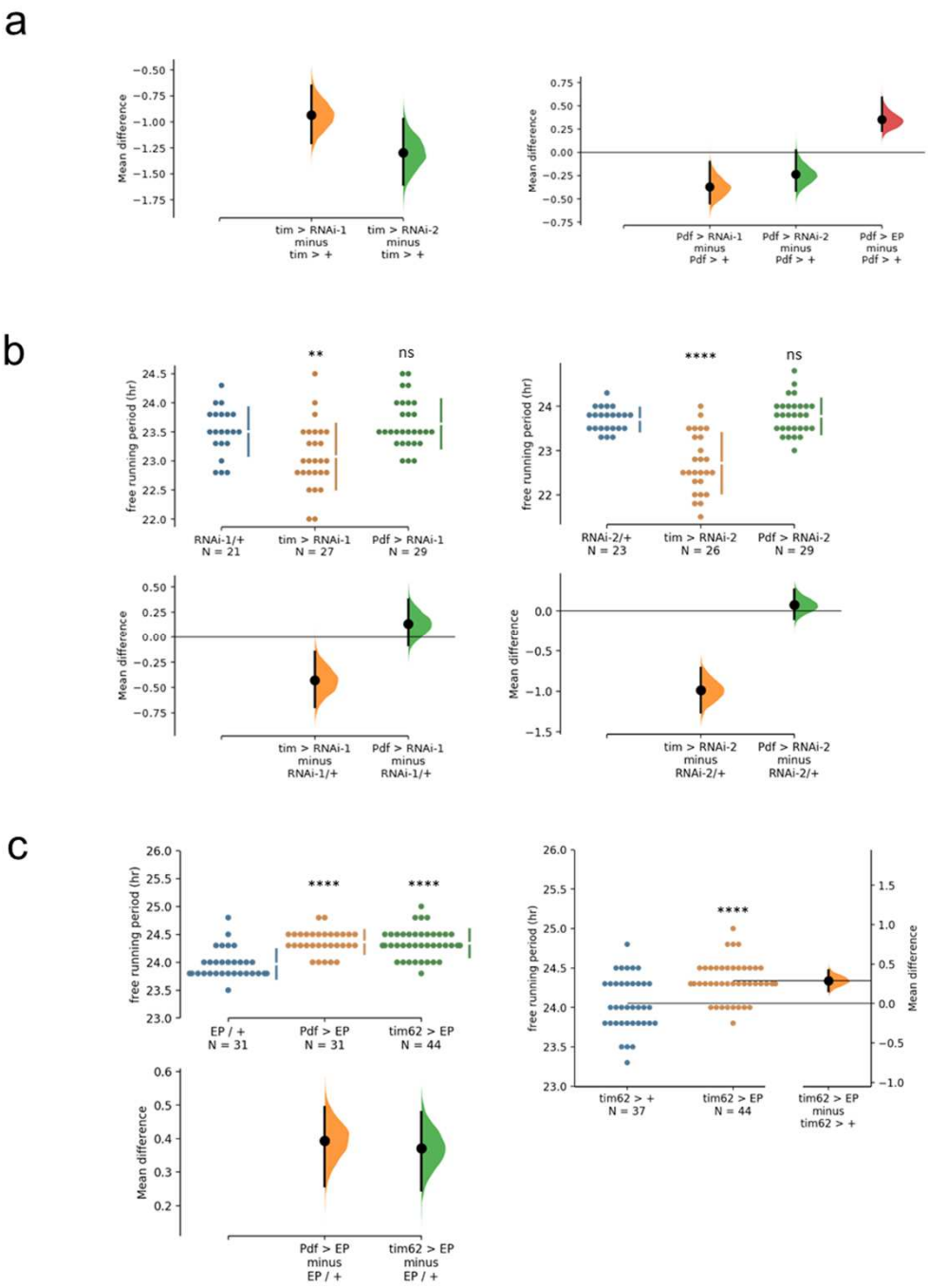

Supplemental Fig. S5. Statistical analysis of differences between control flies and those downregulating (A,B) or overexpressing (C) *Drosophila* PPP4R2r. (A) Refers to data shown in **Figure 4D**. The mean difference for 2 comparisons against the shared controls tim > + (left) and Pdf > + (right) are shown as Cumming estimation plot below. Mean differences are plotted as bootstrap sampling distributions. Each mean difference is depicted as a dot. Each 95% confidence interval is indicated by the ends of the vertical error bars. **(B)** The individual period values of the indicated genotypes are plotted on the upper axes (colored dots). The mean ± standard deviation are shown as vertical colored lines and the mean is indicated as a gap in the line. RNAi-1: UAS-PPP4R2r-RNAi TRiP BL26296, RNAi-2: UAS-PPPR2r v105399), tim: tim-gal4:27 UAS-Dicer, Pdf: Pdf-gal4. The mean difference for 2 comparisons against the shared control RNAi-1/+ (left) and RNAi-2 /+ (right) are shown as Cumming estimation plot below. On the lower axes, mean differences are plotted as bootstrap sampling distributions. Each mean difference is depicted as a dot. Each 95% confidence interval is indicated by the ends of the vertical error bars. **(C)** Left: Same as (B), genotypes EP: P{EP}PPP4R2rEP307, Pdf: Pdf-gal4, tim62: tim-gal4:62. Note that the UAS-Dicer construct is not present in this line. Right: colored dots show individual period lengths. The mean difference between tim62 > + and tim62 > EP is shown in the above Gardner-Altman estimation plot. Both groups are plotted on the left axes; the mean difference is plotted on a floating axes on the right as a bootstrap sampling distribution. The mean difference is depicted as a dot; the 95% confidence interval is indicated by the ends of the vertical error bar. P values were determined by Students t test: **** $P < 0.00005$, ** $P < 0.005$, ns = not significant.

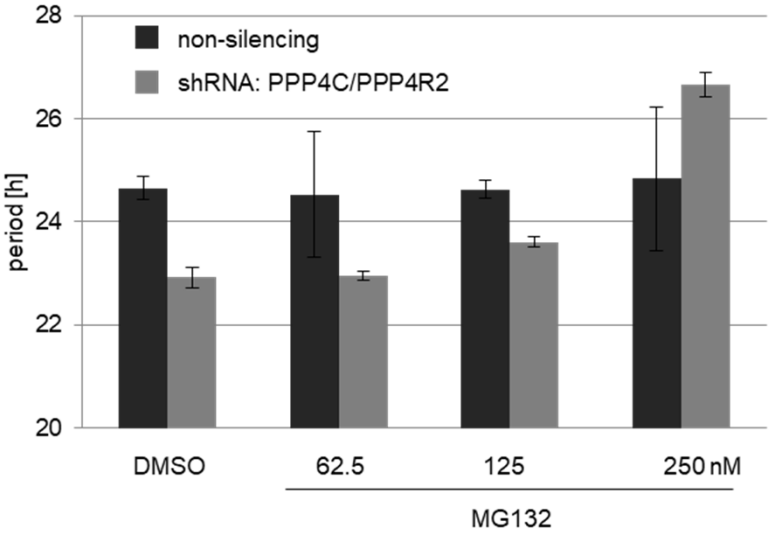

Supplemental Fig. S6. PPP4's effect on the circadian period depends on proteasomal activity. Dexamethasone-synchronized U-2 OS reporter cells stably expressing RNAi-constructs targeting PPP4C and PPP4R2 (or a non-silencing control) were treated with indicated concentrations of the proteasomal inhibitor MG132 (or solvent DMSO). Bioluminescence rhythms were monitored for five to seven days in a luminometer. Shown are the mean periods (± SD) of three independent cultures per condition.

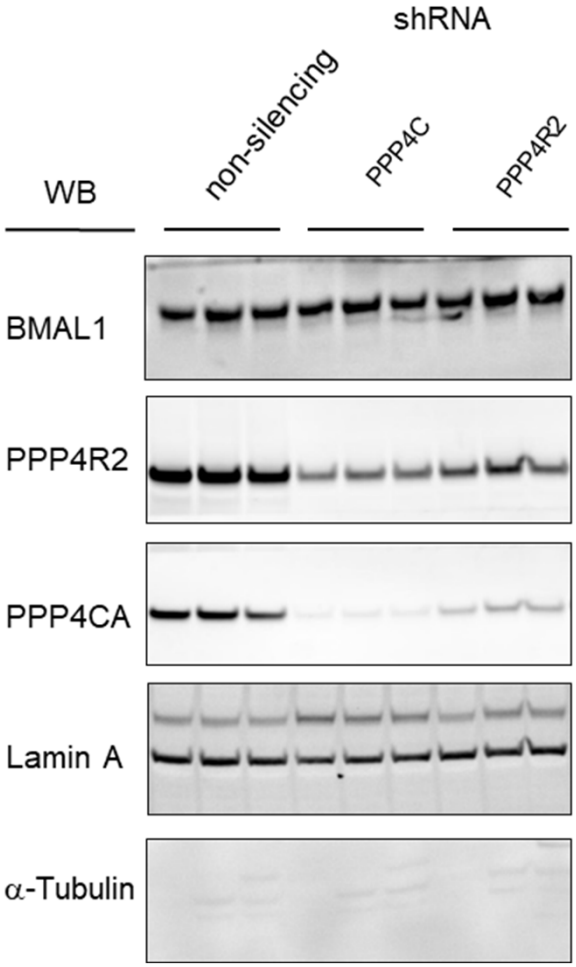

Supplemental Fig. S7. Nuclear BMAL1 levels are unaffected in PPP4C- and PPP4R2-depleted U-2 OS cells. U-2 OS cells were lentivirally transduced with a non-silencing control or with RNAi-constructs targeting *PPP4C* or *PPP4R2*. Shown are Western blots of three independent nuclear extracts each indicating (i) BMAL1 levels are unaffected by PPP4 knockdown, (ii) PPP4 subunits are depleted in RNAi-treated cells and (iii) nuclear extracts show high purity (Lamin A is a nuclear marker and α-Tubulin is a cytosolic marker).

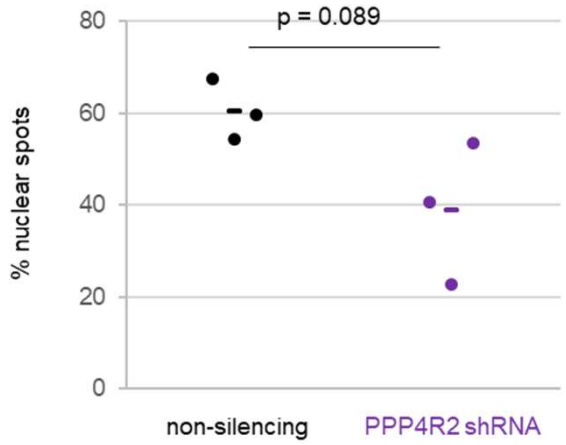

Supplemental Fig. S8. CLOCK/BMAL1 occupancy on target promoters is modulated by PPP4. BMAL1-YFP binding to *Dbp* gene arrays in murine NIH3T3 cells (Stratmann et al., 2012) with our without knockdown of PPP4R2 was analyzed using fluorescence microscopy experiments. Shown are the numbers of fluorescent nuclear spots per cells analyzed in three independent experiments. These spots correspond to BMAL1-YFP binding to *Dbp* gene arrays. *P* value was determined by Students t-test.

Genotype	N	% rhythmic	tau (h) ± SEM	RS ± SEM
tim-gal4:27 UAS-Dicer/+	30	100	24.0 ± 0.1	4.4 ± 0.2
tim-gal4:62/+	37	100	24.0 ± 0.1	4.4 ± 0.2
Pdf-gal4/+	30	100	24.0 ± 0.1	5.5 ± 0.2
PPP4R2r RNAi-1 (TRiP BL26296)/+	23	91	23.5 ± 0.1	3.3 ± 0.3
PPP4R2r RNAi-2 (v105399)/+	24	96	23.7 ± 0.1	3.7 ± 0.3
EP307 (P{EP}PPP4R2r^{EP307})/+	31	100	24.0 ± 0.1	5.1 ± 0.3
tim27>dicer>PPP4R2r RNAi-1	27	100	23.1 ± 0.1	2.5 ± 0.2
tim27>dicer>PPP4R RNAi-2	28	93	22.7 ± 0.1	2.7 ± 0.3
tim62>PPP4R2r RNAi-1	31	97	23.4 ± 0.1	2.5 ± 0.2
tim62>PPP4R2r RNAi-2	32	94	23.3 ± 0.1	4.2 ± 0.2
tim62>EP307	44	100	24.3 ± 0.1	4.5 ± 0.2
Pdf>PPP4R2r RNAi-1	32	91	23.6 ± 0.1	3.5 ± 0.2
Pdf>PPP4R2r RNAi-2	30	97	23.8 ± 0.1	5.1 ± 0.2
Pdf>EP307	31	100	24.4 ± 0.1	5.8 ± 0.3

Supplemental Table S1. Free-running period values of locomotor activity recorded from male flies with the indicated genotypes in DD at constant 25 °C. Period values (tau) were determined by autocorrelation. Rhythm Statistics (RS) indicates the robustness of the activity rhythms. In this study, all flies with RS values ≥ 1.5 were considered rhythmic (see Methods).